American Society of Agricultural and Biological Engineers

An ASABE Meeting Presentation

Paper Number: 062207

Assessment of SEBAL model for estimating evapotranspiration in the Devils Lake basin

[1]Ramesh Gautam; [2]Dean Steele; [3]David Hopkins; [4]Mike Sharp

[1, 2]Agricultural and Biosystems Engineering Department, North Dakota State University, Fargo, ND 58105

[3, 4] Soil Science Department, North Dakota State University, Fargo, ND 58105

Written for presentation at the
2006 ASABE Annual International Meeting
Sponsored by ASABE
Oregon Convention Center
Portland, Oregon
9 - 12 July 2006

Abstract Above-average rainfall in the last twelve years has led to rising water levels in the Devils Lake basin in northeastern North Dakota. An irrigation test project has been started at ten farmer-cooperator field sites within the basin to estimate how much additional water can be utilized via irrigation of agricultural crops. Comprehensive soil/water compatibility investigations coupled with GIS analysis of detailed soil survey data (SSURGO) will be utilized to assess the potential for sustainable irrigation development and potentially extend the results to the entire basin. The installation and monitoring phase of the test project will be described in this paper. Water balance monitoring at the sites will include measurements of rainfall and irrigation, soil water content, deep percolation, and ground water level. The surface energy balance algorithm for land (SEBAL) model will be developed in Erdas Imagine/Arc Map interface for estimating evapotranspiration (ET) in the basin. Correlations will be developed between ET and soil physical and chemical properties affecting sustainability as well as other factors, such as crop types, soil map units, and landscape position in order to assess the feasibility, impact, and sustainability of the larger scale irrigation in this mostly non-irrigated basin.

Keywords. Devils Lake Basin, Irrigation, Water Utilization, Energy Balance, Evapotranspiration, SEBAL, Soil/water compatibility, LANDSAT

INTRODUCTION

Devils Lake basin, located in the north-eastern part of North Dakota, is also one of the basins where the consistent pattern of excessive rainfall has caused the Devils lake water level to continuously rise since 1995. The impact of the rising water level has tremendous adverse implications at the vicinity of the Lake.

In this study, the effective utilization of surface water resources for irrigation of cultivable land in upper Devils Lake basin is being investigated. By utilizing the surface water resources for various crops, e.g., corn, wheat, and soybeans, the water from the Devils Lake basin could have been properly used to uplift the economic conditions of the region by improving the crop yield. Moreover, the water will also be effectively utilized for vegetables for maximizing the yield. In addition, equal attention has also been drawn not to degrade the soil salinity. Hence, the study has been encompassed to timely monitor the soil as well as surface and sub-surface movement of salts in the farm fields. Moreover, by constructing several control stations, the nature of the soil properties will be examined to evaluate the impact of the sprinkle irrigation in the basin.

Surface energy balance algorithm for land (SEBAL) will be coded in Erdas Imagine software in window platform to exploit the information from the Landsat 5 TM satellite image. All visible bands, NIR band and the thermal band of the satellite image will be used to estimate various components of the surface energy balance algorithm. Moreover, the study will be further expended to develop simulation and prediction based mathematical models as well as neural network based models to infer the spatial and temporal patterns of the surface water within the basin. Moreover, sub-pixel based algorithms will be utilized and expanded to analyze the satellite images that may have partial cloud cover. Suitable clustering algorithms will be developed to define the area with cloud content and with non cloud content, which will be helpful to decide the type of the image application in the study area. Also, the time and spatial extent of the satellite images will be observed to find the trade off between the temporal scale and spatial scale of the satellite image.

The literature shows that various techniques have been adapted at several places in the world to estimate the evapo-transpiration at a basin scale. Recently applied remote sensing techniques are getting popularity because of several reasons. Of course one of the reasons is because of the availability of spatial patterns of the vegetation and soil data in the form of spectral radiance at different spectral bands of electromagnetic spectrum. The reflected source of energy from the vegetation is captured at different spectral band, which is extracted and processed using suitable mathematical algorithms to estimate spatial and temporal patterns of ET from the basin. Of course much credit goes to Bastiaanssen (1995, 1998a, 1998b, 2000), who identified the algorithm and applied it to measure various components of surface heat fluxes from the earth surface and tested the algorithm at diverse climatic conditions at various parts of the world. Ayenew (2003) presented surface energy balance algorithm for land (SEBAL) approach to calculate daily evaporation of some of the Ethiopian rift lakes and the surrounding landscape from the thematic mapper spectral satellite data. His study demonstrates that evaporation from a single lake varies depending upon surface temperature, albedo and on the incoming fluxes from groundwater and surface water bodies. The variation in

evaporation ranged from 4.9 to 5.9 mm/day from the lakes. On the land surface, actual evapo-transpiration increases with altitude following the availability of moisture in the soil instead of the temperature gradient. On average it ranges from 0.2 mm/day in rift lacustrine soils and salty lake shores to around 4.5 mm/day in the highland mountain peaks covered with afro-alpine vegetation. His study clearly indicates the differences in evapo-transpiration based on vegetation types and altitude of the area under consideration. It also hinted at the careful application of numerous parameters in mountainous regions when applying the SEBAL algorithm.

French et al., (2005) applied multispectral thermal and near infrared band ASTER images to accurately estimate surface energy fluxes from space at high spatial resolution which has the potential to improve predictions of the impact of land-use changes on the local environment and to provide a means to assess local crop conditions. They adapted a combination of physically based surface flux models and high-quality remote-sensing data to yield surface temperature, vegetation cover, and land-use types. They applied the algorithm to demonstrate the usability of the algorithm to retrieve the data over an experimental site in central Iowa, USA. They considered two different flux estimation approaches, which were: (i) Two-Source Energy Balance model (TSEB); and (ii) Surface Energy Balance Algorithm or Land model (SEBAL). The study showed that the ASTER data were sufficient to have spatial and spectral resolution in order to derive surface variables required as inputs for physically based energy balance modeling. Both TSEB and SEBAL were found to have systematic agreement and responded to spatially varying surface temperatures and vegetation densities.

Bastiaanssen et al., (2005) depicted the major principles of SEBAL and summarized the accuracy of the model under several climatic conditions at both field and basin scales. For a range of soil wetness and plant community conditions, the typical accuracy at field scale was found to be 85% for 1 day and 95% on a seasonal basis. On the other hand, the accuracy of annual ET of large watersheds was found to be 96% on average.

Study objectives

The objectives of the study are to:

- Determine how much additional surface water in the Devils Lake basin can be utilized via sprinkler irrigation of agricultural crops compared with non-irrigated crops.
- Evaluate the effects of irrigation on representative soil map units within the basin.
- Extrapolate results from the test project to estimate the total volume of water that could be prevented from entering Devils Lake through extensive development of irrigation in the basin.

STUDY AREA

Devils Lake Basin is located in northeastern North Dakota, USA (Figure 1). The entire basin covers about 3814 square miles (2,44,0960 acres). The geographical boundaries of the basin are 99^{o} 47’ west and 99^{o} 4’ west longitude; 47^{o} 46’ north and 49^{o} 0’ north

latitude. The basin encompasses portions of nine counties; Ramsy, Towner, Pierce, Benson, Eddy, Nelson, Walsh, Rolette, and Cavalier (Figure 2). The basin is a typically non contributing portion of the Red River of the North's drainage area. There are nine sub-basins within the basin which are connected via natural coulees. Mauvais stream originates along the southern flanks of the Turtle mountains 90 to 120 m above the elevation of Devils Lake and enters Big Stream at Lake Irvine. Big Stream flows from Lake Irvine into Devils Lake's west bay. The Edmore, Starkweather, St. Joe, and Calio streams originate in southern Cavalier County and flow in a south-southwesterly direction. Little stream serves about 421 square miles on the west side of the basin and joins Big Stream approximately 5 miles from Churches Ferry.

Devils Lake basin topography is glacial in origin with low hills and flat lands. Many depressions, wetlands, small lakes and pools are connected via poorly defined natural drainage system. The studies show that the chains of lakes are important factors affecting the flow of water into Devils Lake (North Dakota State Water Commission, 2005). It is also known that about 86 percent of run off from the basin goes to Devils Lake. The remaining 14 percent contributes to Stump Lake located in the southeast portion of the basin.

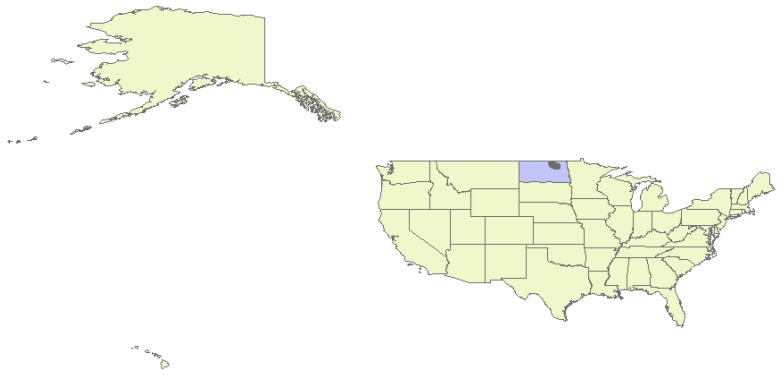

Figure 1 Location of the Devils Lake Basin

Flooding occurs when the runoff occurs in the area which is nearly level in topography. The well developed upper basin drainage system leading into the chain of lakes carries water more quickly than the lakes system can effectively manage it. The uncontrolled water flowing into the flat area typically causes overland flow. Management of these lakes may help diminish flooding both around the lakes and downstream.

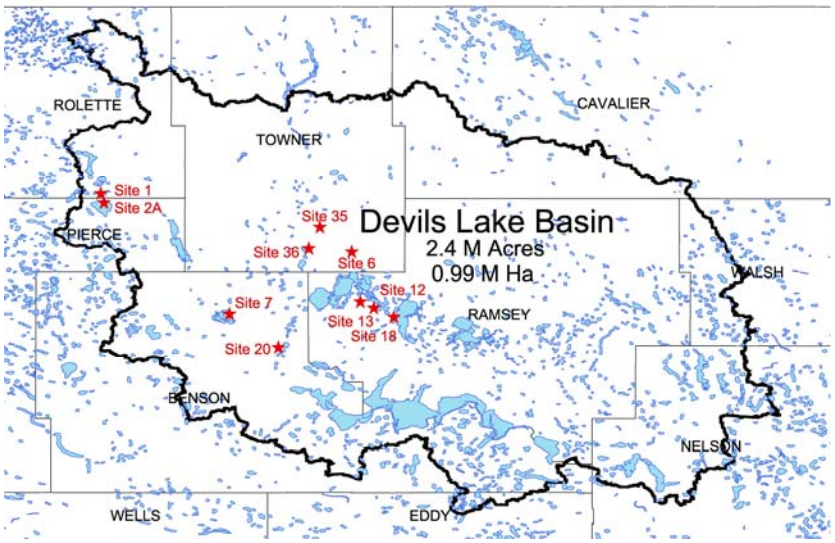

Figure 2 Location of the test sites in Devils Lake Basin

Selection of test sites

Initial investigation was performed to select potential irrigation test sites at various locations within Devils Lake basin. Based on the location, topography, soil type, geo morphology, natural slope, drainage patterns, vegetation, and county representation, ten sites were selected for installation of pivot irrigation systems. Two sites (sites 1 and 2A) are located each in Rolette and Pierce County. There are three sites (sites 35, 36, and 6) in Towner County. Similarly three sites (sites 12, 13, and 18) are located in Ramsey County and there are two sites (sites 7 and 20) in Benson County. Figure 2 shows the location of the ten sites in the Devils Lake basin.

INSTRUMENTATION

Pivot irrigation systems were installed at all ten sites. Depending on the topography, field boundaries, crop type, and drainage patterns, some center pivots are allowed to rotate in a full circle and some are not. The scope and length of the pivot irrigation system also differs from site to site depending on the coverage area. The objectives of installing such systems are to utilize the water from nearby surface waters to irrigate crops during summer of project years. Utilizing scientific irrigation scheduling scheme, the pumps will be operated at an specified interval with pre-specified pumping rate to irrigate the field. Various crops were planted at different sites. For example, site 1, 2A, 6, 12, and 13 were planted with corn in year 2005, sites 7 and 18 were planted with half soybeans and half corn, site 35 was planted with half cabbage and half corn, site 36 with half corn and half pumpkins, and site 20 was with alfalfa. It is also important to note that the cropping systems will be rotated with other crops in the project years i.e., in 2006 and 2007. Moreover, water samples were collected from pivot irrigation system to analyze surface water quality for constituents relevant to soil and water compatibility investigations, e.g., sodium, calcium, magnesium, electrical conductivity etc. Figure 3 shows a typical pivot irrigation system installed at one of the ten sites.

Figure 3 Pivot Irrigation systems at alfalfa site (site 20)

Rain gauge installation and monitoring

Both manual and tipping bucket rain gauges were installed at the beginning of summer each year in 2005 and 2006. The rain gauges will be installed in the year 2007. Daily rainfall data have been collected from all tipping bucket rain gauges using Watchdog data loggers (Spectrum Technologies, Inc, Plainfield, Illinois). Manual rain gauges were emptied once every one to two weeks. The manual rain gauges record the data for a minimum of one inch interval. A typical installation of manual and tipping bucket rain gauges is shown in Figure 4.

Figure 4 Installation of manual and tipping bucket rain gauge

Flux meter installation

Twenty five flux meters were installed at ten sites varying from one to four in each site. The location and number of flux meters were determined based on soil map units representative of those in the basin. The objectives of installing flux meters were to record the intensity and volume of water percolated through the vadoze zone in a time series manner. Initially, distinct soil types were identified using reconnaissance survey. Based on the area of coverage and dominancy of the soil types, the locations of flux meters were fixed. Using global positioning system (GPS), these locations were recorded in Arc Pad and subsequently to desktop Arc GIS for future references. The flux meters were constructed in the Agricultural and Biosystems Engineering Department laboratory at North Dakota State University. These prototypes were tested in the lab mimicking similar field conditions in order to ensure the proper recording of rate and volume of water percolated from the field. Then, the flux meters were transported into the field.

Initially, about eight feet bore holes were dug at most of the sites. The depth varied depending on crop type, root zone and ground water level. Then, various soil horizons were identified for the same depth nearby the bore hole in test pits. Using manual soil sampling equipment, soil samples were taken at each soil horizon. Then, the density of in-situ soil types was determined. The fluxmeters were filled with similar soil types at respective levels to mimic the natural soil strata in fluxmeters. The top level of the flux meter was set at the bottom of crop root zone at each site. Hence, depending on the crop type, the depth of the top level of flux meter was set below the surface. As shown in Figure 5, various soil strata were identified and the amount of soil required for specific depth was collected from nearby soil pit. The flux meters were filled with corresponding soils accordingly. Figure 6a and 6b show subsequent steps of flux meter installation in the field.

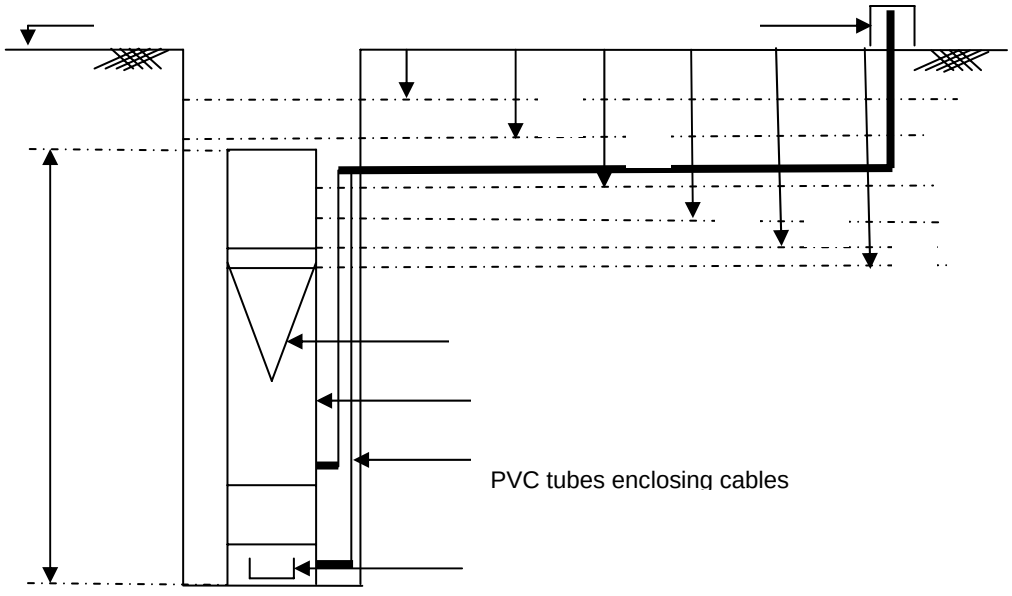

Figure 5. An example of fluxmeter installation in the field with various soil types and strata. Each alphabet indicates distinct soil layers or horizons.

Figure 6a Sequential steps of flux meter installation in the field

Figure 6b Sequential steps of flux meter installation in the field

Soil characterization and sampling

Soil characterization has been performed at each site to determine the chemical constituents in the soil in vertical vadoze zone. Three cores were extracted from each station. The depth of cores varied from 1.78 to 2.79 m depending on the morphology of the sites. These cores were brought to the soil science laboratory and then the analysis of cations and anions was performed at each depth at an interval of 10 cm. As shown in Figure 7 the soil core characterization sampling stations were given names of A, B, and C.

Figure 7 Each hole is corresponding to soil characterization and sampling

Neutron probe readings

Neutron probe readings were performed at each station to monitor the soil moisture content at various depths in the vertical profile. The access tubes were installed at each station with the help of probe truck and then the neutron probe was normalized with the shield readings. The calibrated probe was used to record the readings at each 6 inch depth interval. The readings were plotted against the soil moisture determined from the laboratory for the corresponding station. Figure 8 illustrates a probe and reading devices in the field.

Figure 8 Neutron probe readings for soil moisture monitoring

Installation of monitoring wells

Eighteen shallow ground water monitoring wells were installed at ten sites varying from one to three per site depending on the site conditions, soil types, and morphology. The objective of the observation well installation was to monitor the time series variation of ground water level in each site. Moreover, the water samples collected from each site will be analyzed to determine chemicals like nitrate, phosphate, bicarbonate, chloride, etc. In selected cases where shallow ground water is expected to contribute to ET we plan to monitor diurnal water table fluctuations to quantify this component of ET. Figure 9 illustrates a typical observation well installed at one of our monitoring sites.

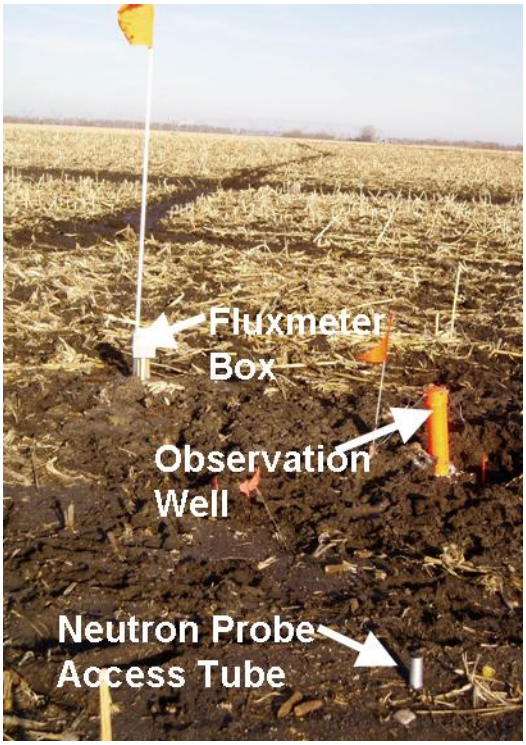

Figure 9 Instrumentation at one of the test sites

Installation of weather station

Computation of evapo-transpiration requires calibration and validation of several parameters, such as sensible heat flux, and soil heat flux. In order to compute the heat flux components meteorological data are required to be collected at the time of satellite over pass. Therefore, one of the sites was selected for weather station installation and monitoring purposes. The selection of the site was made based on alfalfa crop, suitability of the landscape, and fulfilling the requirements for space and widening of the site considering wind direction, vicinity of lakes and trees. Air temperature and relative humidity sensors were installed at three different elevations from the surface. The first sensor was put about 75 cm above the surface, the second and third sensors were installed at about 1 and 1.5 m above the surface. The purpose of recording air temperature and relative humidity at different levels was to compute the momentum

roughness length. Other sensors installed at the station were near infrared sensor, solar radiation sensor, wind speed and direction sensor, and tipping bucket rain gauge sensor. The weather station is based on a Campbell Scientific (Logan, Utaha) CR10x data logger equipped with a cellular phone to transfer data to the soil and water laboratory in the Agricultural and Biosystems Engineering Department, North Dakota State University. The data are being collected at ten minute, one hour and twenty-four hour intervals. Figure 10 shows the set up of the weather station.

Figure 10 Weather station installed at alfalfa site, near Devils Lake, North Dakota

THEORETICAL PRESPECTIVE

Landsat 5 TM visible as well as thermal band images will be used to estimate evapotranspiration in the Devils Lake basin. Incoming short wave radiation, long wave radiation, outgoing long wave radiation, sensible heat flux, and soil heat flux are estimated in addition to the surface albedo and emissivity of the atmosphere. The following mathematical equation is used to estimate the net heat radiation. The algebraic sum of net heat radiation, soil heat flux and sensible heat flux provide the latent heat radiation. The latent heat flux is used to estimate the evapo-transpiration (Bastianssen et al., 2000).

$$R_n = (1-\alpha)R_S \downarrow + R_L \downarrow - R_L \uparrow - (1-\varepsilon_o)R_L \qquad (1)$$

$$R_n = G + H + \lambda ET \qquad (2)$$

Acquiring satellite image

LANDSAT TM-5 satellite image of the research sites will be collected once in every two weeks starting from May 2006 to October 2007. There are two satellite scenes that cover the entire basin. The path and row of the satellite scenes are 26/32 and 26/33. Our plan is to collect visible, near infrared, and thermal band of Landsat 5 image and then develop an algorithm to extract surface albedo. The surface albedo will be used to

estimate various components of incoming solar radiation. The mathematical equations will be used to estimate the evapo-transpiration using satellite images. Following components of solar radiations are computed using empirical equations and/or with the help of other parameters applied in this study.

Short wave radiation

Solar radiation incoming at the earth's surface constitutes short wave radiation and long wave radiation. The short wave radiation when incident at the top of the atmosphere has multiple reflections due to atmospheric aerosols and other gases at the atmosphere. The fraction of reflected solar radiation also falls at the surface due to phenomena of multiple reflections. The downward component of solar radiation striking at the surface is given by the amount reduced by the albedo of the land surface ie, $Q_s=Q_{clear}(1-\alpha)$. The incoming radiation can be computed from the equations given in Smithsonian Meteorological Tables (1966), with attenuation by clouds as in Reed (1977). The formula for the calculation of short wave radiation is (Rosati and Miyakoda, 1988).

$$Qs=Q_{clear}\ (1-0.62n+0.0019\beta)\ (1-\alpha) \quad (3)$$

Where Q_s is short wave radiation measured in Watt/m^2. n is the cloud fraction taken from field observation and α is albedo of the atmosphere. The parameter $Q_{clear,}$ the incident radiation under clear skies, is composed of direct and diffuse components of short wave radiation, which is,

$$Q_{clear}=Q_{dir}+Q_{diff} \quad (4)$$

The direct component of short wave radiation is

$$Qdir=Q_0\ \tau^{secz} \quad (5)$$

Where the atmospheric transmission coefficient τ = 0.7 (Smithsonian meteorological table) which is considered as a standard value in the normal conditions. z is the zenith angle of the sun which is calculated from

$$z=\cos^{-}(\sin\varphi\sin\delta+\cos\varphi\cos\delta\cosh) \quad (6)$$

Q_0 is the incident radiation at the top of the atmosphere. The diffused component of net short wave radiation is

$$Q_{diff}=[(1-A_a)Q_0-Q_{dir}]/2 \quad (7)$$

Where A_a=0.09 is the absorption due to water vapor and ozone (Smithsonian meteorological table, 1966). β is solar noon altitude which is calculated in degree as

$$\beta=\sin^{-}(\sin\delta\sin\varphi+\cos\delta\cos\varphi\cosh) \quad (8)$$

Where δ is declination of the sun, which is calculated from

$\delta=\sin^{-}(\sin\varepsilon\ \sin\gamma)$ where ε is obliquity of ecliptic, (23.439-0.0000004N) and γ is longitude of the place under consideration. Considering the spherical coordinates, the longitude of the place is computed from (L+1.915sing+0.020sin2g) where, L is mean longitude and g is anomaly of the sun. The mean longitude and anomaly are computed by L=

(280.46+0.9856003N) and g = (357.528+0.9856003N) (Atlas of surface marine data 1994). N is number of days from Julian day (Ist January 2000) = (JD-2451545). The Julian day is computed from

JD = (367Y-7(Y+(M+9)/12)/4+275M/9+D+1721013.5+UT/24. Where, Y is the year, M is month, D is the day and UT is universal time of observation. φ is the latitude of the place and h is the hour angle of the sun in degree which is calculated as h = $\cos^{-}(-\tan\delta\tan\varphi)$, (Atlas of surface marine data). The direct solar radiation at the top of the atmosphere is calculated from

$$Q_0 = J/\pi(E_0)^2[h(180/\pi)\sin\varphi\sin\delta+\cos\varphi\cos\delta\cosh) \quad (9)$$

Where E_0 is eccentricity correction factor which is computed as

E_0=1.00011+0.034221cosη+0.00128sinη+0.000719cos2η+0.000077sin2η where η=2π(D-1)/365 where D is the calendar day number. J is solar constant (1367 watt/m^2/k^4). The flow chart below gives the overall procedure to comute short wave radiation. Program was written in C to compute the short wave radiation.

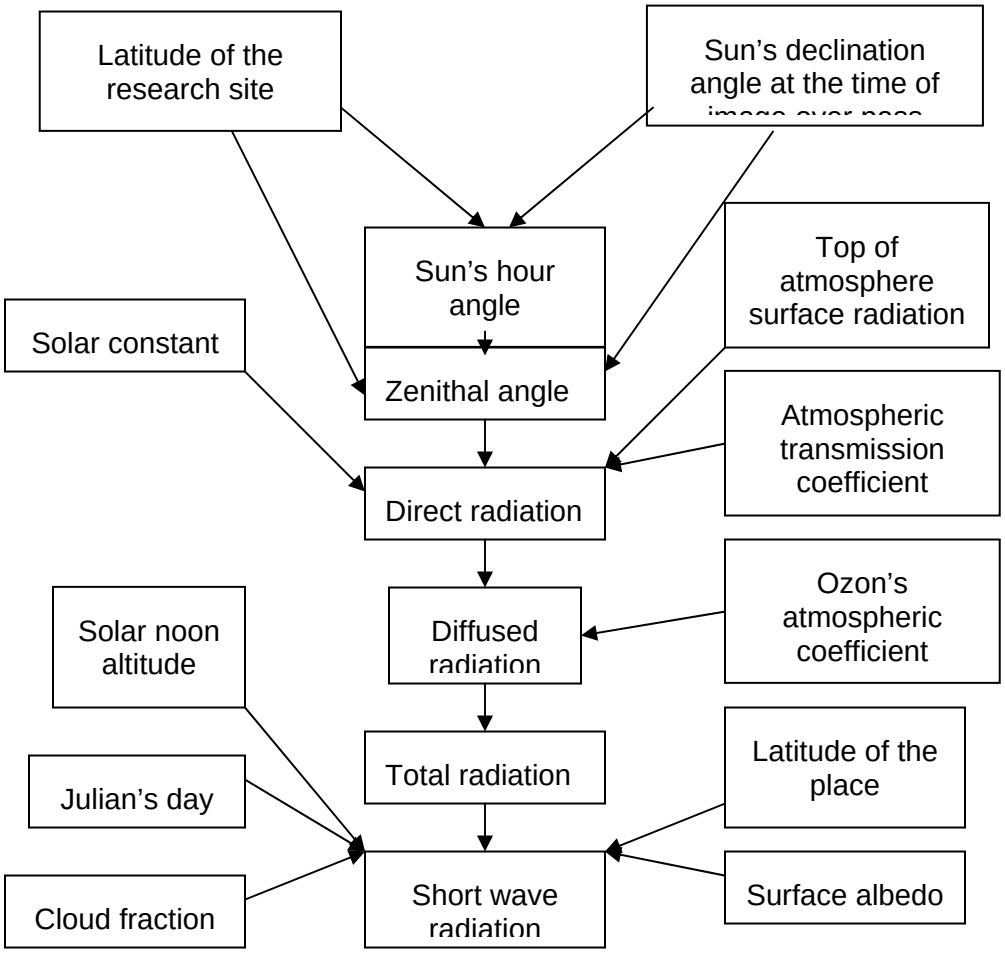

Figure 11 Step by step process to compute short wave radiation

Incoming long wave radiation

The downward thermal radiation flux from the atmosphere constitutes long wave radiation. Long wave radiation can be computed using Stefan-Boltzmann equation as follows:

$$Q_{long}^{in} = \varepsilon \sigma T_a^4 \qquad (10)$$

Where ε is the atmospheric emissivity, σ is Stefan-Boltzmann constant, and T_a is the near surface air temperature. The emissivity is normally calculated using the following equation.

$$\varepsilon = 0.85(-\ln \tau_{sw})^{0.09} \qquad (11)$$

Figue 12 illustrates the computation of incoming long wave radiation. The long wave radiation is estimated in Erdas Imagine software using the spatial modeler language of the model maker tool.

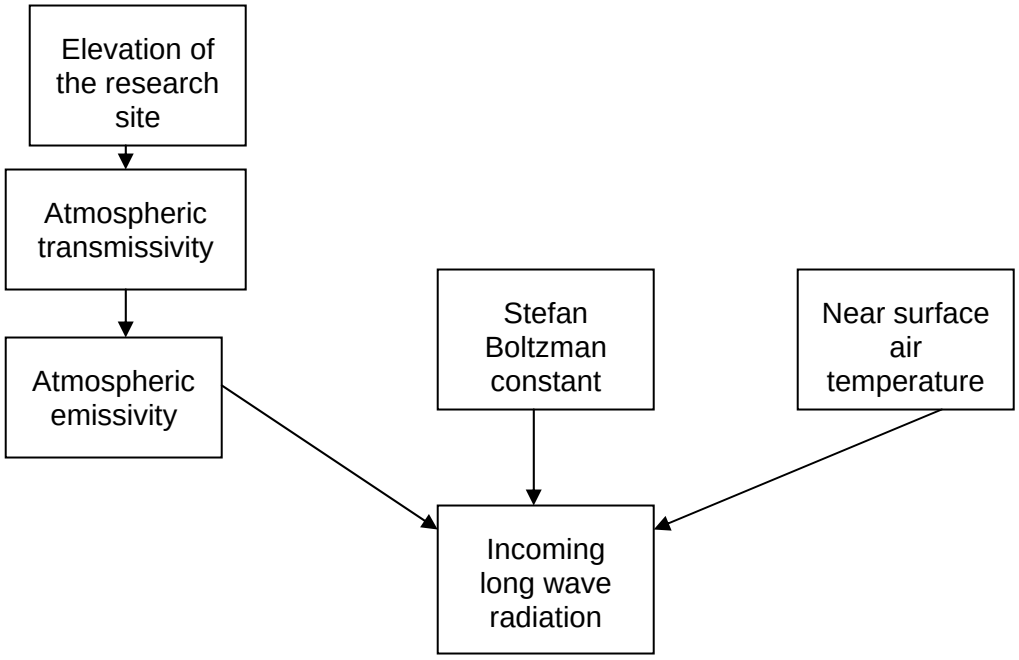

Figure 12 Process to compute incoming long wave radiation

Outgoing long wave radiation

The outgoing long wave radiation is the thermal radiation flux emitted from the earth's surface to the atmosphere. The empirical formula used to compute outgoing long wave radiation is a simple modification of Gill (1982).

$$Q_{long}^{out} = \varepsilon T_a^4 (0.39 - 0.05 e_a - 0.5)(1 - \chi n_c^2) + 4\varepsilon \sigma T_s^3 (T_s - T_a) \qquad (12)$$

Where Q^{out}_{long} is the long wave radiation measured in Watt/m^2. The dimensionless cloud coefficient χ varies with latitude (Oberhuber, 1988). But for the particular latitude,

its value can be assumed to be constant (Kleeman and Power, 1992). ε is emissivity of the surface, which is calculated using equation 9 and σ is Stefan's Bolotzman's constant (5.67×10^{-8}). e_a is water vapor pressure at near land surface. It can be computed from observed air pressure at the weather station. n is cloud content. T_s and T_a are the land surface and air temperatures, respectively. For this study, normalized difference vegetation index (NDVI), soil adjusted vegetation index (SAVI), leaf area index (LAI), surface emissivity (ε), thermal band radiance, and clear sky solar radiation are used to compute outgoing long wave radiation. The flow chart below shows the outgoing long wave radiation. The algorithm has been coded in Erdas Imagine using model maker tool.

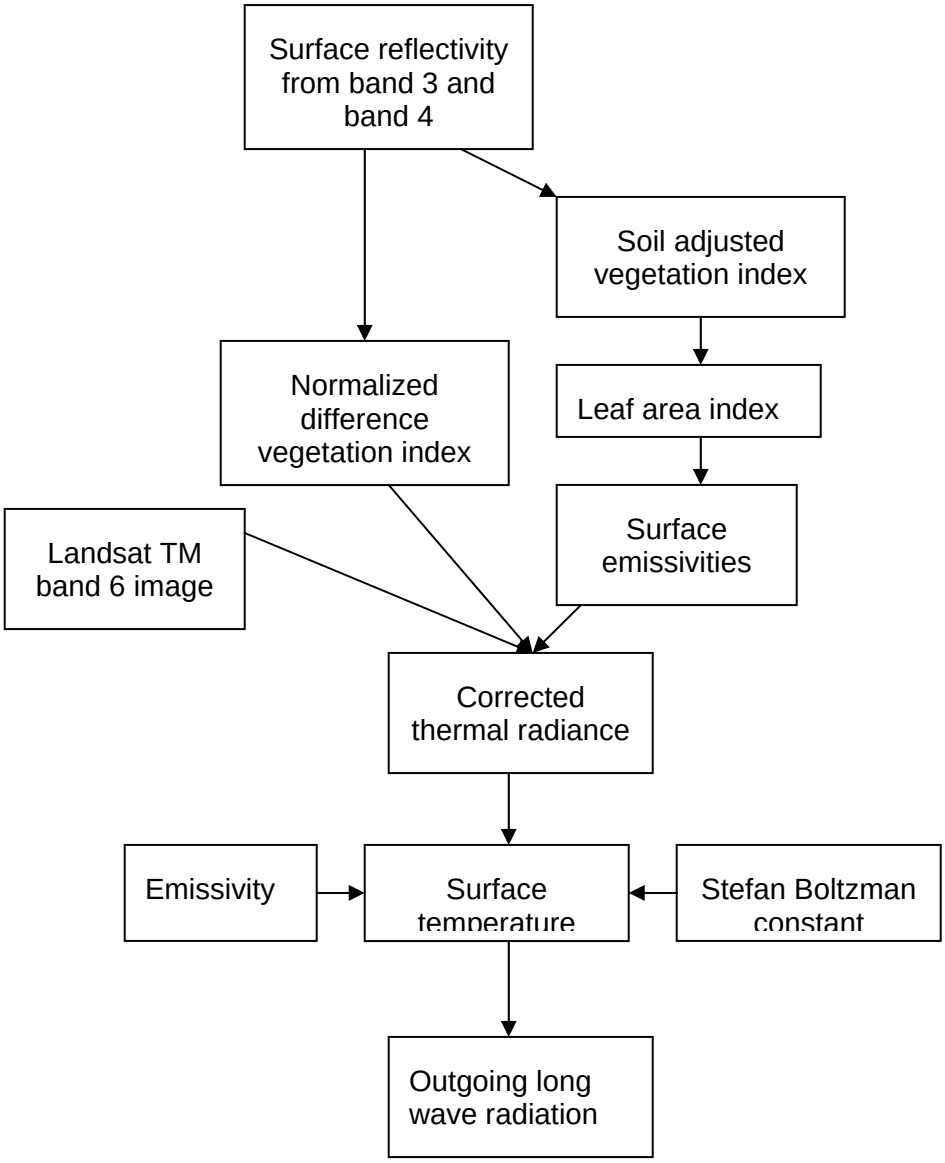

Figure 13 Flow chart to compute outgoing long wave radiation

Soil heat flux

Soil heat flux is a critical component of the surface energy balance along with net radiation, latent heat flux, and sensible heat flux. It is a rate of heat storage in the soil and vegetation due to conduction. Surface energy balance algorithm utilizes NDVI, surface albedo, and surface temperature to compute the ratio of soil heat flux to net solar radiation. Land classification and vegetation type will affect the soil heat flux. The following equation is used to compute the ratio of soil heat flux to net solar radiation.

$$\frac{G}{R_n} = \frac{T_s}{\alpha}\left(0.0038\alpha + 0.0074\alpha^2\right)\left(1 - 0.98NDVI^4\right) \qquad (13)$$

The flow chart below was used to estimate the soil heat flux.

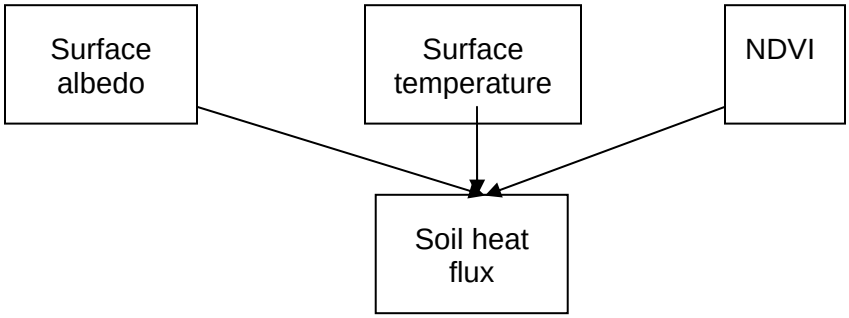

Figure 14 Sequential processes to compute soil heat flux using Landsat images

Sensible heat flux

The temperature difference attributed between the earth surface and the atmosphere constitutes sensible heat flux. It is computed using the following equation.

$$H = \left(\rho c_p \Delta T / r_{ah}\right) \qquad (14)$$

Where ρ is air density; $c_{p,}$ air specific heat, and ΔT is the temperature difference between two heights and r_{ah} is the aerodynamic resistance to the heat transport. The flow chart shows the calculation procedure for the sensible heat flux.

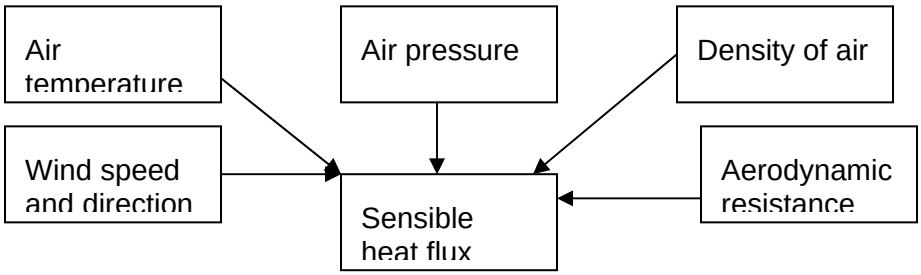

Figure 15 Process to compute sensible heat flux variation at the research sites

Calculation of surface albedo

Surface albedo is a critical component to estimate outgoing long wave radiation. Moreover, surface albedo is a determinant for quantification of evapotranspiration from the vegetation and soil surface. Figure 16 was applied to estimate surface albedo in the Erdas Imagine software.

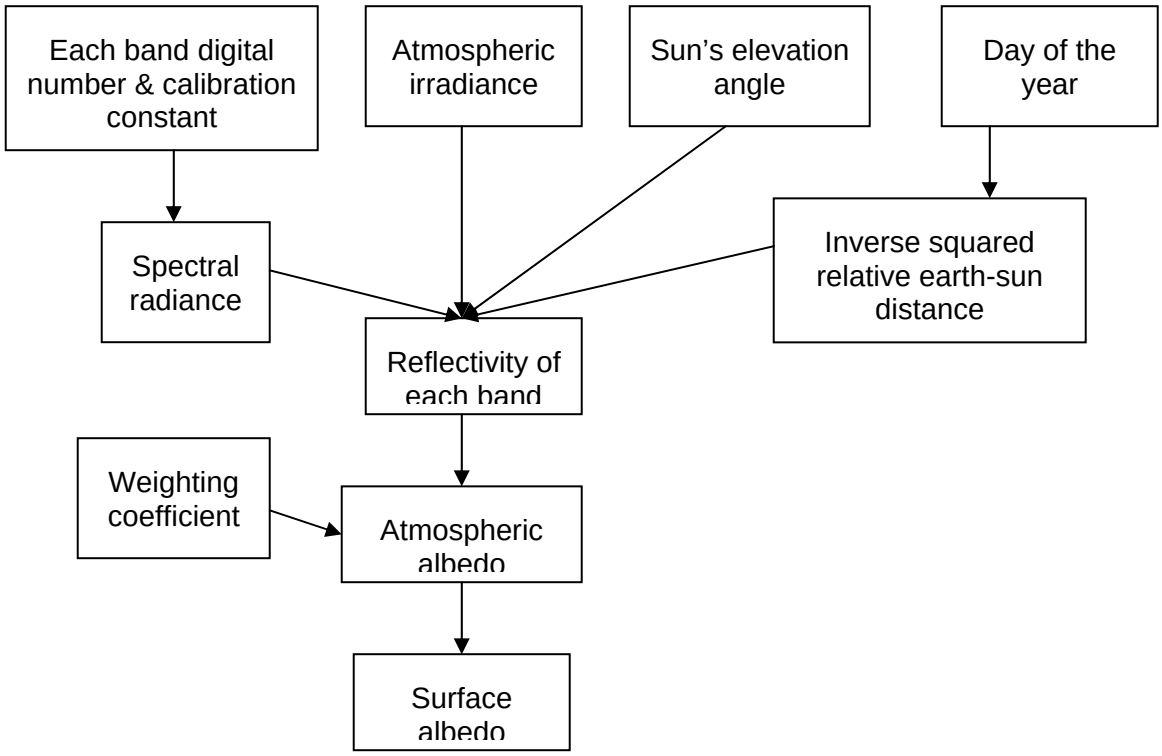

Figure 16 Step by step process to comute surface albedo in Erdas Imagine software using satellite image

Net surface radiation flux

Net surface radiation flux is the mathematical formulation among incoming short wave radiation, long wave radiation, outgoing long wave radiation, surface albedo, and surface emissivity. The following equation is used to compute the net surface radiation flux in surface energy balance algorithm (Bastianssen et al., 2000).

$$R_n = (1-\alpha)R_{s\downarrow} + R_{L\downarrow} - R_{L\uparrow} - (1-\varepsilon_o)R_{L\downarrow} \qquad (15)$$

Where R_n is net surface radiation; R_s-incoming short wave radiation; R_L-incoming and outgoing long wave radiation; α-surface albedo; ε_o- surface emissivity.

Instantaneous Evapotranspiration

An instantaneous value of evapo-transpiration in equivalent evaporation depth is computed using

$$ET_{inst} = 3600 \frac{\lambda ET}{\lambda} \qquad (16)$$

Where ET_{inst} is the instantaneous ET and 3600 is time conversion factor to hours. λ is the latent heat of vaporization. The reference ET is defined as the ratio of the computed instantaneous ET for each pixel to the reference ET computed from weather data. Similarly, daily values of ET are computed by multiplying the reference ET fraction with 24 hours reference ET. The seasonal ET map can be derived from the 24 hour evapo-transpiration data by extrapolating the ET_{24} proportionally to the reference evapotranspiration (ET_r).

RESULTS AND DISCUSSIONS

Time series patterns of rainfall data

Rainfall data collection was begun since May 2005. Tipping bucket and manual raingauges were used to record daily rainfall patterns at all ten research sites. The data were collected (will be collected) between May and October each project year. An instance of rainfall patterns at one of the test sites is shown below. Rainfall pattern indicates that the month of June, 2005 was rainy month.

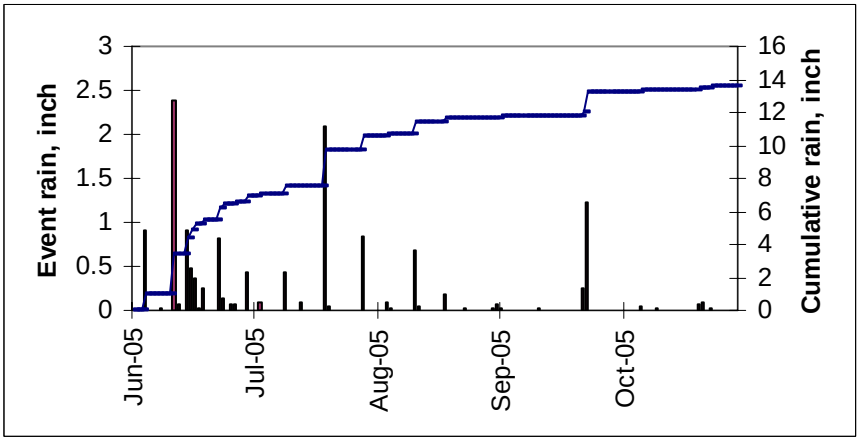

Figure 17 Rainfall patterns between June and October, 2005 at site 12, Devils Lake basin, North Dakota

Calibration of neutron probe readings

Neutron probe was calibrated to estimate soil moisture content in vertical vadoze zone at each station in all research sites. Initially, the access tubes were installed into the ground. The soil samples were collected at the three inch depth interval. These soil samples were brought to the laboratory at North Dakota State University and the soil moisture content was determined. Again, the neutron probe was calibrated against the shield readings. Then, the probe was lowered at each six inch increment. The probe readings were recorded. Then a plot was drawn between the soil moisture content (%)

versus probe readings. This was done at each station of all sites. Figure 18 shows the relations between the soil moisture content (%) and the probe readings.

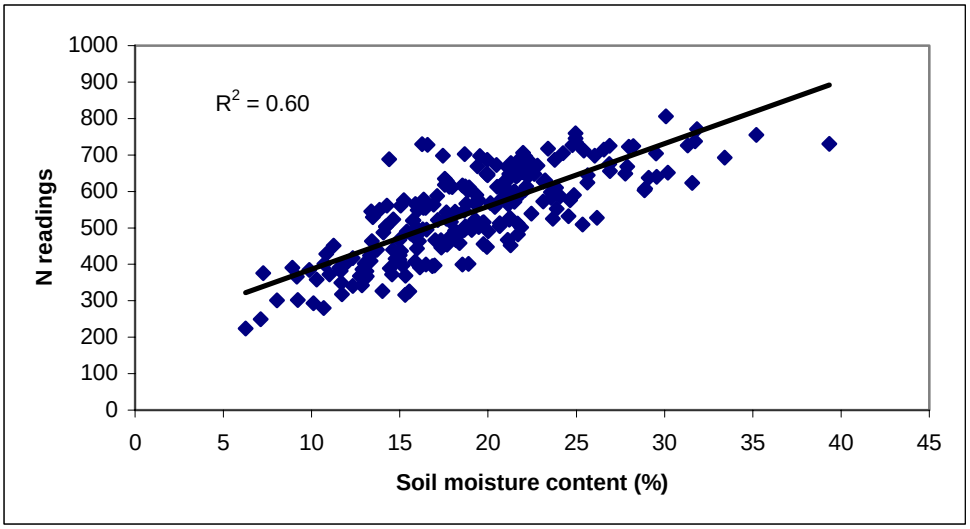

Figure 18 Relations between soil moisture content and neutron probe readings

Algorithm formulation

The components of net wave radiation were determined in Erdas Imagine software in window PC. The following Minot site images located in Minot, North Dakota, USA, were derived in Erdas Imagine as a sample image. Each image is corresponding to different components of the surface heat balance algorithm.

Figure 19 A portion of a Landsat 7 TM image reflecting albedo at Minot research site, Minot, North Dakota

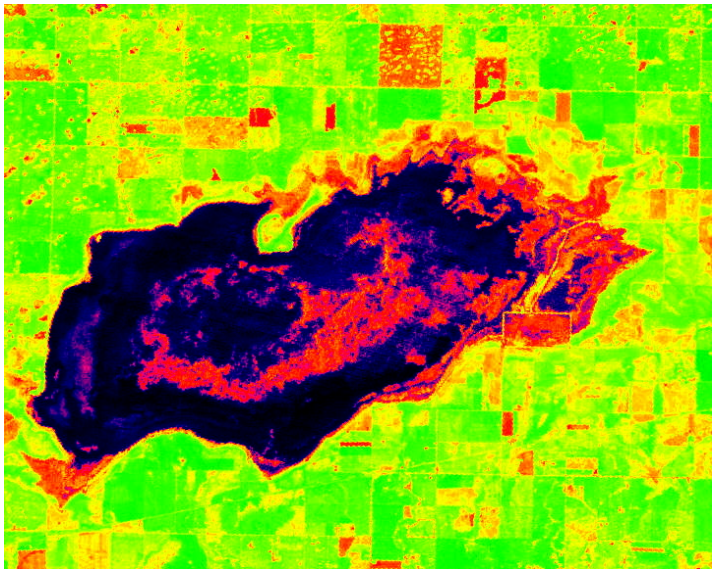

Figure 20 A sample of NDVI map of the Minot research site

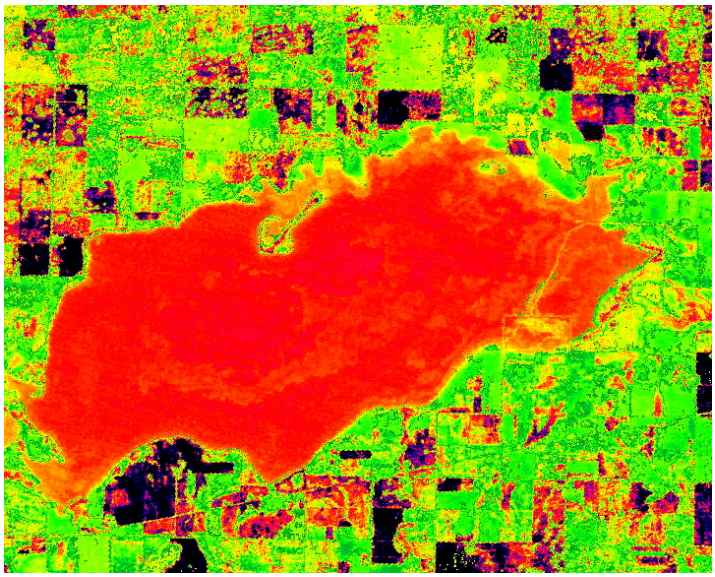

Figure 21 Soil heat flux, a portion of Landsat image over Minot research site, Minot, North Dakota

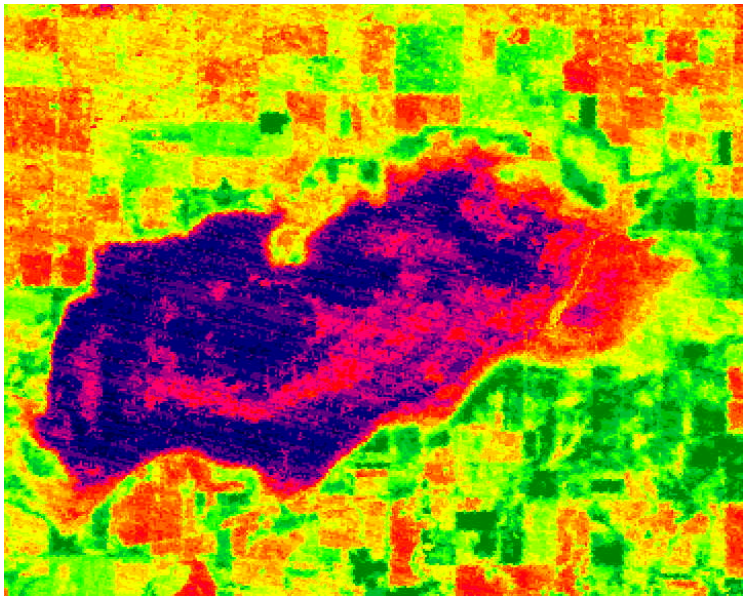

Figure 22 Surface temperature of a Minot research site

Conclusions

An initial phage of the test project has been completed. Twenty five flux meters, eighteen observation wells, twenty five neutron access tubes, ten manual and tipping bucket raingauges each, and a meteorological stations were installed in the sites. Initial development of the algorithm for estimating evapo-transpiration using Landsat satellite image has been completed in Erdas Imagine window platform. Rainfall data collection, laboratory analysis of soil samples, well development, laboratory analysis of water quality parameters are in progress. The calibration of neutron probe access tubes has been completed.

Future plan

Our future plan include analysis of Landsat TM satellite image for estimating evapo-transpiration over the Devils Lake basin, monitoring the fluxmeters, observation wells, rainfall data collection, weather data collection, and analysis of the data. Our future plan also include development of mathematical models for vertical movement of nutrients, development of nutrient zones, sensitivity analysis of different parameters for the water quality variation in the field, synchronization of images for prediction model building to estimate the evapo-transpiration. Application of neural network technique to automate the real time estimation of the evapo-transpiration, use of fuzzy clustering techniques for segmentating cloud images from cloud free images and thus, use of sub-pixel mapping technique to apply thirty percent cloud images for estimating vegetation parameters.

Acknowledgement

Financial and in-kind support has been provided by the Devils Lake Basin Joint Water Resource Board, the North Dakota Agricultural Experiment Station, and the NDSU Carrington Research Extension Center.

References

Atlas of surface marine data (1994). disc1: directly observed quantities, disc2: heat, water and fresh water fluxes, u.s department of commerce, NOAA, NODC.

Ayenew, T. (2003). Evapo-transpiration estimation using thematic mapper spectral satellite data in the Ethiopian rift and adjacent highlands, Journal of Hydrology, 279, 83-93.

Bastiaanssen, W. G. M., M. Meneti, R. A. Feddes, and A. A. M. Holtslag, (1998a). A remote sensing surface energy balance algorithm for land (SEBAL): 1. Formulation., Journal of Hydrology, 212-213, 198-212.

Bastiaanssen, W. G. M., H. Pelgrum, J. Wang, Y. Ma, J. Moreno, G. J. Roerink, and T. Van der wal, (1998b). A remote sensing surface energy balance algorithm for land (SEBAL): 2. Validation. Journal of Hydrology, 212-213, 213-229.

Bastiaanssen, W. G. M. (2000). SEBAL based sensible and latent heat fluxes in the irrigated Gediz Basin, Turkey. Journal of Hydrology, 229, 87-100.

Bastiaanssen, W. G. M, E. J. M. Noordman, H. Pelgrum, G. Davids, B. P. Thoreson, and R. G. Allen (2005). SEBAL model with remotely sensed data to improve water resources management under actual field conditions. Journal of Irrigation and Drainage Engineering, ASCE 131 (1): 85-93

Chow et al. (1988). Applied hydrology, international edition, McGrow-Hill Book Company pp. 58

French, A. N., F. Jacob, M. C. Anderson, W. P. Kustas, W. Timmermans, A. Gieske, Z. Su, H. Su, M. F. McCabe, F. Li, J. Prueger, N. Brunsell, (2005). Surface energy fluxes with the advanced Spaceborne Thermal Emission and Reflection radiometer (ASTER) at the Iowa 2002 SMACEX site (USA). Remote Sensing of Environment, 99, 55-65.

Gill, A., 1982. Atmospheric-ocean dynamics, *Int.Geophys. Ser*, vol. 30, Academic Press, 662.

Kleeman, T., and S. B. Power, 1995. A simple atmospheric model for surface heat flux for use in ocean modeling studies, Journal of physical oceanography, vol. 25, pp: 92-105.

Overhuber, J., 1988. An Atlas based on the CODAS Data Set: The budget of heat buoyancy and turbulent kinetic energy at the surface of the global ocean. (Report No. 15), Max-Planck Institute for Meteorology.

Reed, R. K., 1977. On estimating isolation over the ocean, Journal of physical oceanography, vol. 7, pp: 482-485.

Rosati, A., and K. Miyakoda, 1988. A general circulation model for upper ocean

Spectrum Technologies Inc., 12360 South Industrial Dr., East - Plainfield, Illinois 60585, http://www.specmeters.com.